

The Novel Imidazopyridine 2-[2-(4-Methoxy-pyridin-2-yl)-ethyl]-3*H*-imidazo[4,5-*b*]pyridine (BYK191023) Is a Highly Selective Inhibitor of the Inducible Nitric-Oxide Synthase

Andreas Strub, Wolf-Rüdiger Ulrich, Christian Hesslinger, Manfred Eltze, Thomas Fuchß, Jochen Strassner, Susanne Strand, Martin D. Lehner, and Rainer Boer

Departments of Biochemistry, Chemistry and Pharmacology, ALTANA Pharma AG, Konstanz, Germany (A.S., W.-R.U., C.H., M.E., T.F., J.S., M.D.L., R.B.); and Department of Internal Medicine, Johannes Gutenberg University, Mainz, Germany (S.S.)

Received July 21, 2005; accepted October 13, 2005

ABSTRACT

We have identified imidazopyridine derivatives as a novel class of NO synthase inhibitors with high selectivity for the inducible isoform. 2-[2-(4-Methoxy-pyridin-2-yl)-ethyl]-3*H*-imidazo[4,5-*b*]pyridine (BYK191023) showed half-maximal inhibition of crudely purified human inducible (iNOS), neuronal (nNOS), and endothelial (eNOS) NO synthases at 86 nM, 17 μ M, and 162 μ M, respectively. Inhibition of inducible NO synthase was competitive with L-arginine, pointing to an interaction of BYK191023 with the catalytic center of the enzyme. In radioligand and surface plasmon resonance experiments, BYK191023 exhibited an affinity for iNOS, nNOS, and eNOS of 450 nM, 30 μ M, and >500 μ M, respectively. Inhibition of cellular nitrate/nitrite synthesis in RAW, rat mesangium, and human embryonic kidney 293 cells after iNOS induction showed 40- to 100-fold higher IC₅₀ values than at the isolated enzyme, in agreement with the much higher L-arginine concentrations in cell culture

media and inside intact cells. BYK191023 did not show any toxicity in various rodent and human cell lines up to high micromolar concentrations. The inhibitory potency of BYK191023 was tested in isolated organ models of iNOS (lipopolysaccharide-treated and phenylephrine-precontracted rat aorta; IC₅₀ = 7 μ M), eNOS (arecaidine propargyl ester-induced relaxation of phenylephrine-precontracted rat aorta; IC₅₀ > 100 μ M), and nNOS (field-stimulated relaxation of phenylephrine-precontracted rabbit corpus cavernosum; IC₅₀ > 100 μ M). These data confirm the high selectivity of BYK191023 for iNOS over eNOS and nNOS found at isolated enzymes. In summary, we have identified a new highly selective iNOS inhibitor structurally unrelated to known compounds and L-arginine. BYK191023 is a valuable tool for the investigation of iNOS-mediated effects in vitro and in vivo.

NO synthases are enzymes responsible for the generation of nitric oxide from the amino acid L-arginine (for review, see Alderton et al., 2001). Two classes of enzymes exist, which

differ in their activation profile and their capacity to generate NO. Once expressed the inducible NO synthase (iNOS) is active for prolonged periods and produces micromolar concentrations of NO over longer periods. The iNOS expression is stimulated in various cell types by proinflammatory signals and is involved in immune defense against invading pathogens (Stuehr et al., 1991; Schmidt and Walter, 1994; Moncada and Higgs, 1995). The constitutively expressed en-

These studies were supported in part by grants SFB 553 C15 and SFB 432 B6 from the Deutsche Forschungsgemeinschaft (to S.S.).

Article, publication date, and citation information can be found at <http://molpharm.aspetjournals.org>.
doi:10.1124/mol.105.017087.

ABBREVIATIONS: iNOS, inducible nitric-oxide synthase; L-NMMA, N^G-monomethyl-L-arginine; eNOS, endothelial nitric-oxide synthase; L-NIL, N⁶-(1-iminoethyl)-L-lysine hydrochloride; NOS, nitric-oxide synthase; BYK191023, 2-[2-(4-methoxy-pyridin-2-yl)-ethyl]-3*H*-imidazo[4,5-*b*]pyridine; BYK205516, 6-amino-2,4-lutidine; BH₄, 6*R*,6*S*-5,6,7,8-tetrahydro-L-biopterin dihydrochloride; GW273629, (S)-[2-[(1-iminoethyl)amino]ethyl]-4,4-dioxo-L-cysteine; GW274150, (S)-[2-[(1-iminoethyl)amino]ethyl]-L-homocysteine; 1400W, N-[3-(aminomethyl)benzyl]acetamidine; ONO1714, (1*S*,5*S*,6*R*,7*R*)-2-aza-7-chloro-3-imino-5-methylbicyclo[4.1.0]heptane hydrochloride; SC-51, L-N⁶-(1-iminoethyl)lysine-5-tetrazole amide; 2-AP, 2-amino-4-picoline; MES, 2-(*N*-morpholino)ethanesulfonic acid; HEK, human embryonic kidney; DMEM, Dulbecco's modified Eagle's medium; FCS, fetal calf serum; LPS, lipopolysaccharide; RMC, rat mesangium cell line; MTT, 3-(4,5-dimethylthiazol-2-yl)-2,5-diphenyltetrazolium; APE, arecaidine propargyl ester; AMT, 2-amino-5,6-dihydro-6-methyl-4*H*-1,3-thiazine hydrochloride; nNOS, neuronal nitric-oxide synthase; EFS, electrical field stimulation; AR-C102222, 1-(6-cyano-3-pyridylcarbonyl)-5',8'-difluorospiro[piperidine-4,2'-(1'*H*)-quinazoline]-4'-amine hydrochloride; BBS-1, 3-[[[benzo[1,3]dioxol-5-ylmethyl]-carbamoyl]-methyl]-4-(2-imidazol-1-yl-pyrimidin-4-yl)-piperazine-1-carboxylic acid methyl ester; BYK205513, 2-methyl-3*H*-imidazo[4,5-*b*]pyridine; BYK237007, 6-[2-(3*H*-imidazo[4,5-*b*]pyridin-2-yl)-ethyl]-4-methyl-pyridin-2-ylamine; BYK299621, 4-methoxy-2-methyl-pyridine hydrochloride.

dothelial and neuronal isoforms are activated by elevated intracellular Ca^{2+} concentrations and generate nanomolar concentrations of NO for relatively short periods. These isoforms have mainly physiological functions in blood pressure regulation and neurotransmission (Marletta et al., 1998; Alderton et al., 2001). Inducible NO synthase is considered as a proinflammatory enzyme and is activated in acute diseases such as sepsis and septic shock (Titheradge, 1999) and in various chronic inflammatory diseases such as asthma, arthritis, multiple sclerosis, and inflammatory diseases of the gut and intestine (Hobbs et al., 1999; Vallance and Leiper, 2002).

A considerable number of inhibitors structurally related to the substrate L-arginine have been developed, such as N^5 -(1-iminoethyl)-L-ornithine (McCall et al., 1991), L-NMMA (Moore et al., 1996), thiocitrullines (Furfin et al., 1994; Narayanan et al., 1995), or isothiourea derivatives (Southan et al., 1995). However, none of these drugs exhibit distinct isoform selectivity. Because inhibition of the endothelial isoform (eNOS) produces hypertension (Moncada and Higgs, 1995), the pharmaceutical development of highly iNOS-selective inhibitors for therapeutic use is desirable.

Selective inhibition of inducible NO synthase seems to be a promising therapeutic approach for the treatment of the acute and chronic diseases mentioned above. Results of selective inhibitors in animal models of acute and chronic diseases are limited. In fact, only very few selective iNOS inhibitors are available for research, and none has reached approved clinical application (Mete and Connolly, 2003). Data from selective inhibitors available such as 1400W (GlaxoSmithKline, Uxbridge, Middlesex, UK) (Garvey et al., 1997), GW274150 and GW273629 (GlaxoSmithKline) (Young et al., 2000; Alderton et al., 2005), AR-C102222 (AstraZeneca Pharmaceuticals LP, Wilmington, DE) (Beaton et al., 2001; Tinker et al., 2003), ONO1714 (Ono Pharmaceuticals, Osaka, Japan) (Nishina et al., 2001), L-arginine derivatives (SC-51 or L-NIL) (Pfizer Central Research, Sandwich, Kent, UK) (Hansel et al., 2003), and the dimerization inhibitor BBS-1 (Berlex Laboratories, Wayne, NJ) (McMillan et al., 2000; Blasko et al., 2002; Habisch et al., 2003) show promising results in animal models of sepsis, lung inflammation, arthritis, and autoimmune diabetes. Development of some of these compounds into the clinic has been stopped because of toxicity issues (1400W) (Alderton et al., 2005). Others show only limited iNOS/eNOS selectivity (ONO1714) (Nishina et al., 2001).

We have identified and characterized a new compound (BYK191023; Fig. 1) with imidazopyridine structure that shows potent and selective inhibition of inducible NO synthase. BYK191023 is not only a valuable tool for preclinical

research on NO synthases but also a promising candidate for clinical development.

Materials and Methods

Materials

Cell culture material NADPH, FAD, FMN, lactate dehydrogenase, sulfanilamide, *N*-(1 naphthyl)ethylenediamine, and lipopolysaccharide (*Salmonella abortus equi*) were obtained from Sigma (Dreieich, Germany). Cytokines were from Peprotec (London, UK). NOS inhibitors were purchased from Alexis Corporation (Läufelfingen, Switzerland); nitrate reductase was from Roche Diagnostics (Mannheim, Germany). [^3H]L-Arginine (60–80 Ci/mmol) was purchased from GE Healthcare (Little Chalfont, Buckinghamshire, UK). (6*R*,6*S*)-5,6,7,8-Tetrahydro-L-biopterin dihydrochloride (BH_4) was from Schircks Laboratories (Jona, Switzerland).

BYK191023 was synthesized at the Department of Medicinal Chemistry (ALTANA Pharma AG, Konstanz, Germany) by condensation of 3-(4-methoxy-pyridin-2-yl)propionic acid with 2,3-diaminopyridine as described previously (Ulrich et al., 2003). [^3H]BYK191023 and [^3H]2-aminopyridine (2-AP) were obtained by catalytic bromine/tritium exchange of 6-bromo-BYK191023 and 3,5-dibromo-2-AP at GE Healthcare. Specific radioactivities of 21 and 64 Ci/mmol, respectively, were obtained. All other chemicals were from commercial suppliers with highest grade of purity.

The human isoforms of NO synthases were obtained essentially as described previously (Butt et al., 2000) or obtained from TransMIT (Giessen, Germany) after transfection of Sf9 cells with the respective human cDNAs via the baculovirus system. The cytosolic fraction of homogenized Sf9 cells was used for all experiments.

Biochemical Methods

NOS Activity Assay. The enzyme reaction using isolated human NOS isoforms was performed in 96-well microtiter F-plates essentially as described previously (Boer et al., 2000). In brief, the assay was performed in a total volume of 100 μl in the presence of 100 nM calmodulin, 226 μM CaCl_2 , 477 μM MgCl_2 , 5 μM FAD, 5 μM FMN, 1 mM NADPH, 7 mM glutathione, 10 μM BH_4 , and 100 mM HEPES, pH 7.2. Final L-arginine concentrations in the assay were 3 to 5 μM . L-[^3H]Arginine (150,000 dpm/well) was added to the mixture, and the reaction was incubated for 60 min at 37°C. Enzyme reaction was stopped by adding 10 μl of 2 M MES buffer, pH 5.0. Then, 50 μl of the incubation mixture was transferred into an MADP N 65 filtration plate (Millipore, Eschborn, Germany) containing 50 μl of AG-50W-X8 cation exchange resin (Bio-Rad, München, Germany). The flowthrough was collected in Pico scintillation plates (PerkinElmer Life and Analytical Sciences, Boston, MA), and the resin was washed twice with water. The total flowthrough of 125 μl was mixed with 175 μl of Microscint-40 scintillation cocktail (PerkinElmer Life and Analytical Sciences). Scintillation plates were counted in a Micro-Beta (PerkinElmer Wallac, Turku, Finland) scintillation counter, and pIC_{50} values were calculated from concentration-response curves by Prism 3.0 (GraphPad Inc., San Diego, CA).

Radioligand Binding Studies. Radioligand binding experiments were performed in 96-well microtiter plates as described previously (Boer et al., 2000) using ^3H -labeled BYK191023 in a total volume of 100 μl in the presence of 2 mM CaCl_2 , 10 μM BH_4 , 1 mM dithiothreitol, 100 μM NADPH, and 50 mM Tris-HCl, pH 7.4. Radioligand competition experiments with nonlabeled compounds were performed using [^3H]2-AP (250,000 dpm/well) corresponding to a concentration of 18 nM as described previously (Boer et al., 2000). The assay was incubated for 60 min at 37°C and then filtered over GF-C glass fiber filter mats (Whatman, Maidstone, UK) with a cell harvester (Skatron, Lier, Norway). Filters were rinsed with ice-cold incubation buffer without NADPH and BH_4 , punched into scintillation vials, and counted after adding 3.5 ml of UltimaGold scintillation cocktail (PerkinElmer Life and Analytical Sciences).

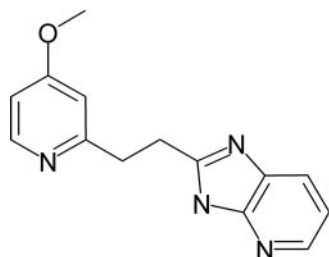


Fig. 1. Chemical structure of BYK191023.

Cytokine-Induced NO Formation in RAW and RMC Cells, NO Formation in HEK293/iNOS Cells. For cell culture, RAW (mouse macrophage cell line; American Type Culture Collection, Manassas, VA) were cultured in Dulbecco's modified Eagle's medium (DMEM), 10% fetal calf serum (FCS), 1% L-glutamine, and 1% penicillin/streptomycin. After reaching confluence, 2×10^5 cells were seeded per well in 96-well microtiter F-plates and stimulated with interferon- γ (100 U/ml) and LPS (1 μ g/ml) in identical serum-reduced media (DMEM, 0.5% FCS, 1% L-glutamine, and 1% penicillin/streptomycin without phenol red). Standard NOS inhibitors in different concentrations were added to the cells, and nitrate and nitrite were determined after 16 h in the cellular supernatant by the Griess assay. Rat mesangium cell line (RMC; American Type Culture Collection) were cultured in RPMI 1640 medium, 10% FCS, 1% L-glutamine, and 1% penicillin/streptomycin. After reaching confluence, the cell line was starved in 96 wells for 48 h in identical serum-reduced media (DMEM, 0.1% FCS, 1% L-glutamine, and 1% penicillin/streptomycin without phenol red) and stimulated with interleukin- 1β (1 nM) in identical serum-reduced media (DMEM, 0.5% FCS, 1% L-glutamine, and 1% penicillin/streptomycin without phenol red). Nitrite was determined after 16 to 20 h in the cellular supernatant by the Griess assay. For culture of HEK293/iNOS cells (Z. Su, J. Kuball, A. P. Barreiros, D. Gottfried, E. A. Ferreira, M. Theobald, P. R. Galle, D. Strand, and S. Strand, submitted for publication), EcR293 cells (human embryonic kidney 293, stably transfected with pVgRXR/Zecocin regulator vector) were grown in DMEM supplemented with 10% FCS, 5% penicillin/streptomycin, 5% L-glutamine, and 5% HEPES buffer at 37°C in a humidified incubator with 5% CO₂. The cDNA of iNOS was cloned into an ecdysone-inducible mammalian expression vector, pIND(SP1)/Neomycin (Invitrogen, Carlsbad, CA). Cells were seeded at 50% confluence and transfected with pIND-NOS2 plasmid by Lipofectamine 2000 reagent according to the supplier's instructions. The stably transfected cells were selected in medium containing both G418 (geneticin) (400 μ g/ml) and Zeocin (400 μ g/ml). Clones growing up after approximately 4 weeks of selection were picked and further analyzed. Cells (10^5) were seeded per well in 96-well microtiter F-plates, and iNOS was stimulated by the addition of ponasterone A (1 μ M; Sigma) for 24 h in identical serum-reduced media (DMEM, 0.5% FCS, 1% L-glutamine, and 1% penicillin/streptomycin without phenol red). Nitrate and nitrite were determined after 24 h in the cellular supernatant by the Griess assay.

For Griess assay, nitrate from 150 μ l of culture media was reduced to nitrite by adding 10 μ l of nitrate reduction buffer (0.08 U/ml nitrate reductase, 530 μ M FAD, and 83 μ M NADPH). Incubation was carried out for 15 min at 37°C in a 96-well microtiter plate. Interfering NADPH was depleted for 5 min at 37°C by addition of mix 2 consisting of 1104 U/ml lactate dehydrogenase and 320 mM sodium pyruvate in a 10- μ l volume. The reaction was abrogated by the addition of 10 μ l of 1% sulfanilamide in 0.1 N HCl and 10 μ l of 0.1% *N*-(1-naphthyl)ethylenediamine. Absorbance was read at 544 nm in reference to 690 nm after a 10-min room temperature incubation in a microplate reader (PerkinElmer Wallac). Nitrite generated from rat mesangial cells was directly assayed in 75 μ l of supernatant by the addition of sulfanilamide and *N*-(1-naphthyl)ethylenediamine.

Determination of Cellular Viability. Cell viability was determined by the MTT assay as described previously (Denizot and Lang, 1986). The cells were washed with phosphate-buffered saline before addition of MTT. Cells were incubated with 100 μ l of 0.2 mg/ml MTT for 90 min at 37°C, 5% CO₂, followed by incubation with 100 μ l of a solution containing 95% isopropanol and 5% formic acid for 10 min at room temperature. Absorbance was read at 544 nm in reference to 690 nm in a microplate reader (PerkinElmer Wallac).

Pharmacological Methods

Isolated Rat Thoracic Aorta: iNOS and eNOS Inhibition. Thoracic aortae were obtained from male Wistar rats (250–300 g; Charles River, Kisslegg, Germany) killed by cervical dislocation. The

vessels were cleaned, cut into rings 1.5 mm in length, and mounted under 0.9- to 1.0-g tension in 10-ml organ baths filled with warmed (37°C), oxygenated (95% O₂, 5% CO₂) Krebs' solution of the following composition: 120.0 mM NaCl, 5.5 mM KCl, 2.5 mM CaCl₂, 1.2 mM MgCl₂, 1.2 mM NaH₂PO₄, 25.0 mM NaHCO₃, and 11.0 mM glucose, additionally containing 10⁻⁵ M indomethacin for the experiments of iNOS inhibition. Isometric tension changes were measured by means of force-displacement transducers and recorded on polygraph recorders. For iNOS inhibition, the endothelium was removed previously by gently rubbing the intimal surface before cutting the vessel into rings that were then placed in Petri dishes containing RPMI 1640 medium containing 200 ng/ml LPS (*S. abortus equi*) and incubated at 37°C for 18 h. This incubation time was chosen from preliminary experiments showing that iNOS expression at the level of mRNA was maximal. The aortic rings were considered denuded when a maximal concentration of the muscarinic agonist, arecaidine propargyl ester (APE; 3×10^{-6} M), caused relaxation of less than 5%. After an initial 60-min equilibrium period, the aortic rings were precontracted by 3×10^{-7} M phenylephrine (EC₈₀₋₉₀ of its own maximal effect), and then 3×10^{-6} M APE (EC₁₀₀) was added to cause rapid relaxation of the tissue within 5 min, before cumulative administration of drugs was started to evoke contraction because of inhibition of eNOS. Likewise, for measuring iNOS inhibition, LPS-treated aortic rings were first challenged with 3×10^{-7} M phenylephrine, which because of iNOS-derived NO caused a partial contraction (5–10% compared with untreated tissue). Thereafter, due to inhibition of iNOS, cumulative administration of test drugs restored the contraction of the hyporeactive tissue. AMT (10⁻⁵ M) was added at the end of the cumulative test drug administration of each NOS inhibitor to define its maximal contractile effect related to that elicited by AMT (100%). All results were expressed as a percentage of the AMT-induced maximal response (Fleming et al., 1990; Eltze et al., 1998).

Field-Stimulated Rabbit Corpus Cavernosum: nNOS Inhibition. Adult New Zealand White rabbits (Dunkin Hartley, 2.5–3.0 kg; Charles River) were sacrificed by intravenous injection of pentobarbital (60 mg/kg) and exsanguination. The penis was dissected free in toto and immediately placed in Krebs' solution. Four longitudinal strips (approximately 1.5 \times 1.5 \times 6 mm) were dissected from each corpus cavernosum and mounted in 10-ml organ baths under a resting tension of 1 g for measurement of isometric tension changes in Krebs' solution: 118.3 mM NaCl, 4.7 mM KCl, 1.9 mM CaCl₂, 1.2 mM MgSO₄, 1.2 mM KH₂PO₄, 25.0 mM NaHCO₃, 0.03 mM Na-EDTA, and 11.1 mM glucose, additionally containing 10⁻⁶ M atropine and 5 \times 10⁻⁶ M guanethidine to exclude possible participation of cholinergic and adrenergic responses, respectively, to electrical field stimulation (EFS). The nutrient solution was aerated with a mixture of 95% O₂ and 5% CO₂ maintaining pH 7.4 at 37°C. The strips were then precontracted by 10⁻⁵ M phenylephrine (EC₈₀₋₉₀ of its own maximal response); after that, relaxant nonadrenergic, noncholinergic responses were evoked by EFS (15 V; 0.3 ms; 4 Hz; for 5 s every 2 min) using a pair of platinum electrodes, one located at the bottom of the organ bath and directly connected with the tissue, and the other ring electrode placed at the top of the bathing fluid. After stabilization of EFS-evoked relaxant responses within 30 to 45 min, the test drug was added in a cumulative manner. The potential inhibition of nNOS could be followed by an inhibition of tissue relaxation mediated by synthesis and release of neuronal NO (Ignarro et al., 1990; Eltze et al., 1999).

Inhibition of iNOS-Derived Nitrate/Nitrite in Rat Aortic Rings. Rat aortic vessels were cleaned and cut into rings 1.5 mm in length. Two rings were transferred into one well in a 96-well plate and stimulated with interferon- γ (100 U/ml) and LPS (1 μ g/ml) for 20 h in serum-reduced media (DMEM, 0.5% FCS, 1% L-glutamine, and 1% penicillin/streptomycin without phenol red). Nitrate and nitrite were determined in the supernatant by the Griess assay as described above.

Statistical Analysis. IC₅₀ values were calculated from inhibition data using Prism 3.0 (GraphPad Inc.). Data presented are mean ± S.E.M.

Results

Identification of BYK191023 as a Novel and Potent Inhibitor of the Inducible Nitric-Oxide Synthase with High Isoform Selectivity. The imidazopyridine BYK191023 (Fig. 1) was identified as a potent inhibitor of iNOS in a biochemical screen using the compound library at ALTANA Pharma AG. NOS activity was measured by quantification of [³H]L-arginine conversion to [³H]L-citrulline. In our NOS activity assays, the K_m values for L-arginine at the three NOS isoforms were determined as 5.7 μM (iNOS), 2.8 μM (nNOS), and 3.3 μM (eNOS) (Boer et al., 2000). BYK191023 consists of an *ortho*-methoxypyridine moiety linked via an ethylene bridge to an imidazopyridine residue. The compound was tested for its NOS inhibitory potency on all three human NOS isoforms. BYK191023 inhibited these enzymes with pIC₅₀ values of 7.03 (iNOS), 4.86 (nNOS), and 3.95 (eNOS) (Fig. 2). Mean pIC₅₀ values (n = 6) for the inhibition of NOS isoforms were 7.07 ± 0.04 (iNOS), 4.79 ± 0.08 (nNOS), and 3.81 ± 0.05 (eNOS), corresponding to IC₅₀ values of 86 nM, 17 μM, and 162 μM, respectively (Table 1). Slope values of inhibition curves were near unity pointing to a homogeneous population of enzyme and an L-arginine competitive mode of action.

L-Arginine Competitive Inhibition of iNOS by BYK191023. Inhibition of iNOS in the presence of increasing L-arginine concentrations led to shifts in IC₅₀ values for BYK191023 shown in Table 2. These data and the resulting linear Schild plot (slope = 1.10; data not shown) point to a stoichiometric relationship between inhibitor and substrate interaction with the enzyme and clearly demonstrate the L-arginine competitive character of binding. To further investigate the molecular mechanism of iNOS inhibition, L-arginine saturation experiments were performed in the absence and presence of increasing concentrations of inhibitor (Fig. 3). Addition of BYK191023 resulted in a shift of the apparent L-arginine K_m value (7.7 μM in the absence and 27, 76, and

129 μM in the presence of 0.3, 1, and 3 μM BYK191023, respectively), whereas the V_{max} of the reaction did not change (Fig. 3A). Analyzing the data in a Schild plot revealed a K_i value for BYK191023 of 85 nM (pK_i of 7.07; intercept with the abscissa; Fig. 3B). A mean K_i value of 90 ± 16 nM was determined in three independent experiments (data not shown). Thus, BYK191023 is a highly potent L-arginine-competitive and -selective inhibitor of the inducible NO synthase.

Structure-Activity Relationships with BYK191023 and Analogs. As can be seen from Fig. 1, BYK191023 consists of two pharmacophore moieties (methoxypyridine and imidazopyridine) linked by an ethylene bridge. To determine the contribution of both pharmacophores to the overall compound inhibitory potency, we synthesized both the methoxypyridine moiety as well as the imidazopyridine residue and analyzed their inhibitory potential at the NO synthases. We were surprised to find that BYK205513, representing the 2-methylated imidazopyridine, exhibited no potency at the NO synthase isoforms (Table 1). In contrast, the 4-methoxy-2-methylpyridine compound BYK299621 showed a micromolar inhibitory potency at the iNOS but no isoform selectivity (Table 1). Combination of both molecules led to the more potent but also highly iNOS-selective inhibitor BYK191023 (Table 1).

TABLE 1

Structure and potency of BYK191023 and analogs at human NOS isoforms (n = 3–6)

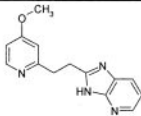
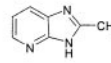
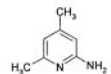
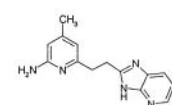
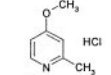
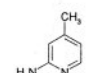
		IC ₅₀		
		iNOS	nNOS	eNOS
BYK191023		86 nM	17 μM	162 μM
BYK205513		>100 μM	>100 μM	>100 μM
BYK205516		102 nM	26 nM	43 nM
BYK237007		55 nM	98 nM	5.6 μM
BYK299621		3.5 μM	5.6 μM	2.6 μM
2-AP		79 nM	68 nM	112 nM

TABLE 2

L-Arginine competitive inhibition of the iNOS by BYK191023 (n = 2)

	L-Arginine			
	16 μM	25 μM	50 μM	100 μM
	μM			
BYK191023, IC ₅₀	0.15	0.45	1.07	2.57

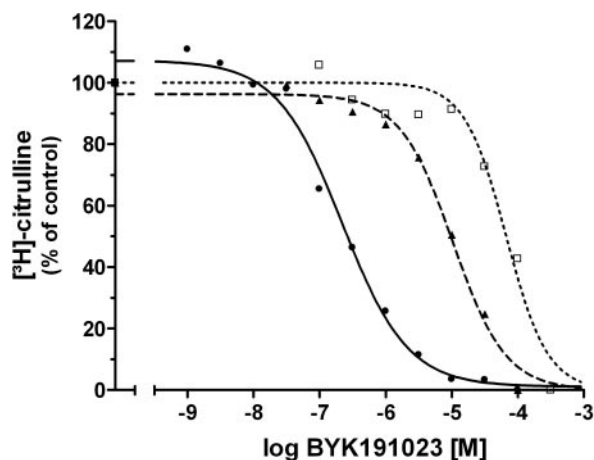


Fig. 2. Inhibition of NO synthases by BYK191023. NOS activation assay was performed with expressed human iNOS (●), nNOS (▲), and eNOS (□) in the presence of the inhibitor BYK191023. pIC₅₀ values of 7.03 M (iNOS), 4.86 M (nNOS), and 3.95 M (eNOS) were obtained for each NOS isoform. Each data point is the mean of duplicate determinations.

Although picolines and aminopicolines are well known as potent NOS inhibitors, they show only minor if any isoform selectivity (Faraci et al., 1996; Boer et al., 2000). As examples, the IC_{50} values of 2-AP and BYK205516 are shown in Table 1. To test whether iNOS selectivity can also be conferred to the 2-aminopicoline moiety by introducing a heteroaromatic residue, we linked the imidazopyridine moiety to the 2-aminopyridine via an ethylene bridge. The resulting compound BYK237007 reveals slightly increased potency compared with BYK191023 and 100-fold selectivity versus eNOS. Selectivity versus the neuronal isoform was low (2-fold) (Table 1).

Affinity of BYK191023 to the Inducible NOS. Thereafter, we analyzed the affinity of BYK191023 toward inducible

NO synthase in radioligand binding experiments using [3 H]BYK191023 as radioligand. Saturation experiments at human iNOS using increasing concentrations of BYK191023 revealed a K_D value for BYK191023 of 1.08 μ M (Fig. 4) and as a mean a K_D value of 1.19 ± 0.06 μ M ($n = 3$). To characterize the [3 H]BYK191023 binding site, radioligand competition experiments using [3 H]BYK191023 as radioligand were performed in the absence or presence of increasing concentrations of standard NOS inhibitors. [3 H]BYK191023 binding was inhibited dose dependently by 1400W, AMT, (S)-ethylisothiourea hydrobromide, and L-NMMA with IC_{50} values of 2.2 μ M, 26.3 nM, 120 nM, and 5.1 μ M, respectively. These binding values correspond well with the inhibition values determined in activity assays (Faraci et al., 1996; Boer et al., 2000).

To further validate the [3 H]BYK191023 binding site as iNOS, we used surface plasmon resonance experiments to measure direct binding of BYK191023 to the highly purified oxygenase domain of murine iNOS. Saturation experiments with BYK191023 using the murine iNOS α protein and BIAcore technology (BIAcore AB, Uppsala, Sweden) revealed a K_D value of 634 ± 81 nM for BYK191023. The association rate amounted to 7200 ± 1600 $M^{-1} s^{-1}$, whereas the dissociation rate was determined as 0.27 ± 0.07 min^{-1} .

Because the low activity of [3 H]BYK191023 against the other two isoforms, especially to eNOS, precludes the use of [3 H]BYK191023 in direct radioligand binding experiments, binding affinities of BYK191023 were determined in radioligand competition experiments using the nonselective NOS ligand [3 H]2-aminopicoline (Table 1). [3 H]2-AP binding to nNOS and eNOS was inhibited at high concentrations with an IC_{50} of 30 and 630 μ M, respectively (Fig. 5). BYK191023 inhibited [3 H]2-AP binding to iNOS in a concentration-dependent manner with an IC_{50} of 450 nM (Fig. 5). Thus, the iNOS selectivity of BYK191023 in binding assays reflects the selectivity previously obtained in activity assays.

Because most in vivo models are performed in rodents, we analyzed the inhibitory potency of BYK191023 at purified murine iNOS to exclude any species related problems. The activity assay was performed as described for the human NO synthases using 5 nM purified murine iNOS. BYK191023 inhibited the murine iNOS with an IC_{50} of 95 nM, compara-

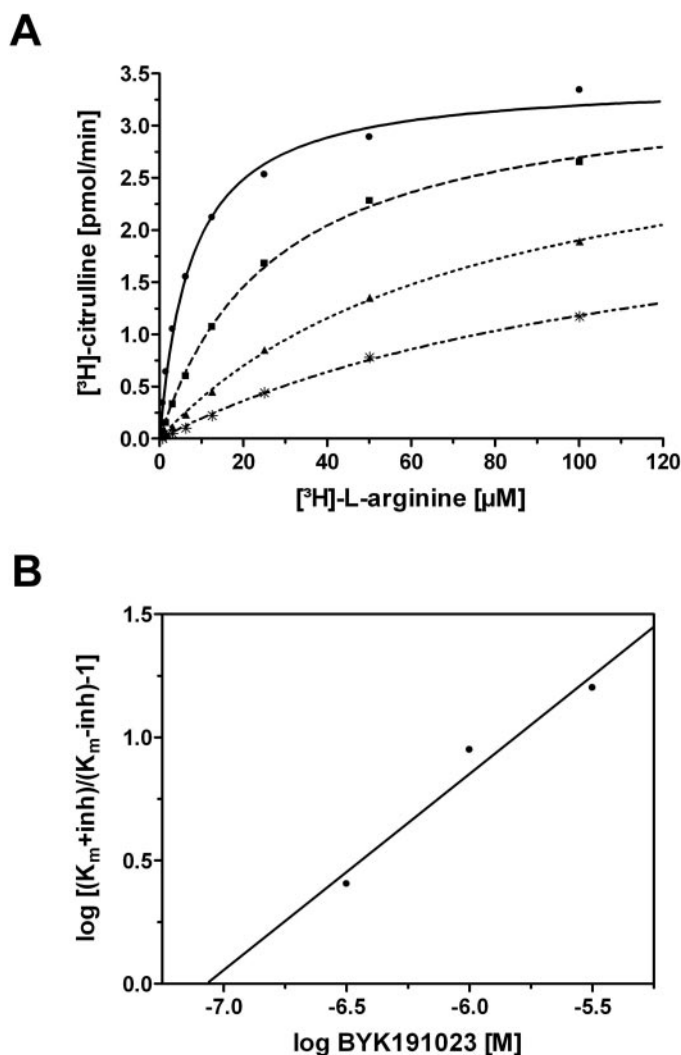


Fig. 3. Substrate dependence of iNOS activity in the presence of increasing concentrations of BYK191023. NOS assay was performed with expressed human iNOS at the indicated concentrations of [3 H]L-arginine in the presence of increasing concentrations of BYK191023. A, saturation plot. Calculated V_{max} values were 3.44 pmol/min in the absence of inhibitor (\bullet), and 3.43, 3.45, and 2.70 pmol/min in the presence of 0.3 μ M (\blacksquare), 1 μ M (\blacktriangle), and 3 μ M ($*$) BYK191023, respectively. The following apparent K_m values were observed for L-arginine: 7.6 μ M in the absence of inhibitor and 27, 76, and 129 μ M in the presence of 0.3, 1, and 3 μ M BYK191023, respectively. B, pK_i value determined by Schild plot. Using the Schild plot (slope = 0.80), the K_i for BYK191023 was determined as 85 nM ($pK_i = 7.07$; intercept with the abscissa). Each data point is the mean of duplicate determinations.

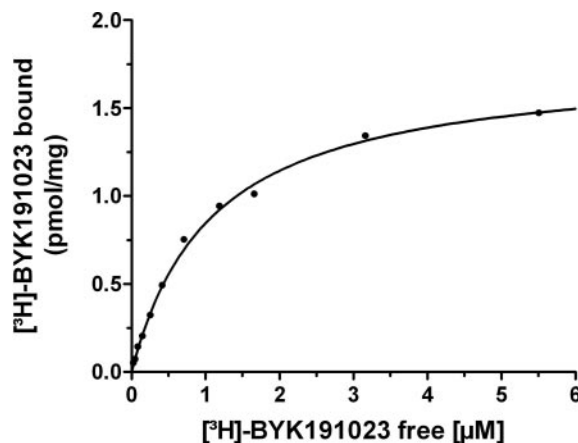


Fig. 4. Saturation isotherm of [3 H]BYK191023 binding to human iNOS. The binding assay was performed with expressed human iNOS and increasing concentrations of BYK191023. An affinity constant (K_D value) of 1.08 μ M was obtained for BYK191023. Each data point is the mean of duplicate determinations.

ble with the potency at human iNOS (86 nM). Furthermore, a highly significant correlation of potencies with various standard inhibitors (including AMT, L-NIL, aminoguanidine, 1400W, N^5 -(1-iminoethyl)-L-ornithine, N^w -nitro-L-arginine methyl ester, and L-NMMA) at the two species was obtained (correlation coefficient $r^2 = 0.87$; $p < 0.001$; data not shown).

Inhibition of iNOS-Derived Nitrite/Nitrate by BYK191023 in Various Intact Cells. The cellular potency of iNOS inhibition by BYK191023 was tested in three cell lines from human, mouse, and rat species. We used the murine macrophage cell line RAW, the rat mesangial cell line RMC, and human HEK293 cells stably transfected with iNOS. Expression of iNOS in these cells was induced either by the addition of cytokines or LPS (RAW and RMC) or by the addition of ponasterone A in the HEK293/iNOS expression system (see *Materials and Methods*). Nitrite generation after induction of iNOS was inhibited by BYK191023 with IC_{50} values of 33 μ M in RMC, 3.1 μ M in RAW, and 13 μ M in human HEK293/iNOS (Fig. 6; Table 3). Addition of 12.5% human serum to the HEK293/iNOS assay led to a small drop in BYK191023 potency (IC_{50} of 28 μ M), possibly because of weak binding of the inhibitor to human serum. Thus, BYK191023 is also a potent inhibitor of the iNOS in various cellular assay systems.

Effect of BYK191023 on Cellular Viability. Cell viability was identified by determination of succinate dehydrogenase activity using the MTT assay. Cells exposed to BYK191023 in all model systems showed no change in their viability. Even at high micromolar concentrations of BYK191023 (100 μ M), cells behaved comparably to control cells in the MTT assay; and in addition, BYK191023 showed no toxicity in hepatocyte tissue cultures up to a concentration of 1 mM (data not shown). Therefore, we conclude that BYK191023 does not exhibit any toxic effect in our cellular models.

Selective Inhibition of iNOS by BYK191023 in Isolated Tissues. We examined the potency and isoform selectivity of BYK191023 in isolated tissues. Pharmacological in vitro models were not only established for determination of

the inhibitory potency at iNOS but also at eNOS and nNOS (see *Materials and Methods*). In vitro models using isolated organs proved to be suitable to determine selectivity of NOS inhibitors. The quality of the models had previously been validated using a number of standard NOS inhibitors (Eltze et al., 1998, 1999).

In LPS-treated rat aortic rings challenged with phenylephrine, due to inhibition of iNOS, cumulative administration of BYK191023 restored the contraction of the hypoactive tissue, resulting in a pIC_{50} value of 5.14. The inhibition curve for BYK191023 reaches a plateau at approximately 70% of the maximal response related to that elicited by 10 μ M AMT (Fig. 7A). To confirm and clarify the reasons for that incomplete inhibition, we measured inhibition by BYK191023 of nitrite generation from LPS-treated rat aortic rings by the Griess assay. A very similar pIC_{50} value of 4.88 was found (Fig. 7B). The experiment was repeated eight times, resulting in a mean pIC_{50} value of 4.90 ± 0.09 . High concentrations of BYK191023 caused almost complete inhibition, showing that the incomplete restoration of the contraction of LPS-treated rat aorta was probably not because of a partial inhibition of inducible NO synthase but must be related to other reasons (e.g., unspecific effects at high concentrations).

The L-arginine competitive inhibition of iNOS in rat aorta by BYK191023 is demonstrated in the original tracing (Fig. 8). BYK191023 (10 μ M) inhibited iNOS and caused contraction of the hyporeactive tissue. Addition of 10 μ M L-arginine antagonized the effect of BYK191023 partially; however, the presence of BYK191023 prevented a complete relaxation. A further increase in BYK191023 concentration (30 μ M) was able to overcome the relaxing L-arginine effect and led to contraction again, which subsequently was attenuated by

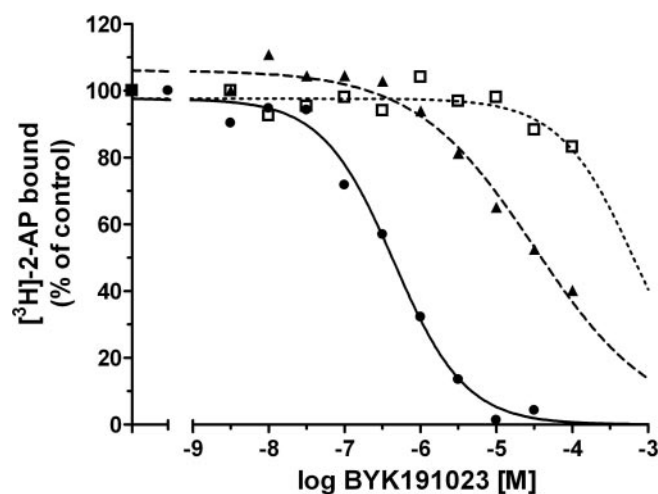


Fig. 5. Inhibition of [3 H]2-aminopicoline binding to human NOS isoforms by BYK191023. The binding assay was performed with expressed human iNOS (\bullet), nNOS (\blacktriangle), and eNOS (\square) as described. BYK191023 inhibited [3 H]2-AP binding to iNOS, nNOS, and eNOS with IC_{50} values of 447 nM, 30 μ M, and 630 μ M, respectively. Each data point is the mean of duplicate determinations.

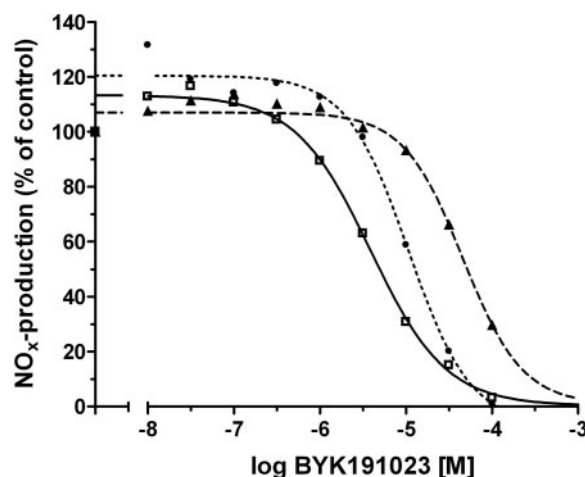


Fig. 6. Inhibition of iNOS in RAW, RMC, and HEK293 cells. The iNOS expression was stimulated and the cellular assays were performed as described using the murine macrophage cell line RAW (\square), the rat mesangial cell line RMC (\blacktriangle), and the HEK/iNOS expression system (\bullet) in the presence of BYK191023. pIC_{50} values of 5.41 M (RAW), 4.34 M (RMC), and 4.97 M (HEK293/iNOS) were obtained for each cell line. Each data point is the mean of duplicate determinations.

TABLE 3
Inhibition of iNOS in various intact cells ($n = 5$)

	RMC	RAW	HEK293/iNOS
	μ M		
BYK191023, IC_{50}	33.0 ± 8.8	3.1 ± 0.5	13.6 ± 4.2

addition of a respective higher L-arginine concentration (30 μ M).

Furthermore, the selectivity of iNOS inhibition by BYK191023 was determined in isolated tissues suitable for determine eNOS and nNOS inhibition. No reversal of APE-induced vasorelaxation by BYK191023 up to 100 μ M was found in phenylephrine-precontracted rat aortic rings as a model for eNOS inhibition (Fig. 7A). In the neuronal NOS model of the phenylephrine-precontracted rabbit corpus cavernosum, BYK191023 showed no inhibition of field stimulation-induced relaxant responses up to concentrations of 100 μ M (Fig. 7A). These data confirmed the isoform selectivity of BYK191023 at the level of isolated organs. In these functional assays, L-NIL showed selectivity for iNOS (pIC_{50} = 6.03) over both eNOS (pIC_{50} = 4.90) and nNOS (pIC_{50} = 4.58), whereas L-NAME behaved as weakly selective for eNOS (pIC_{50} = 5.56) over both iNOS (pIC_{50} = 4.01) and nNOS (pIC_{50} = 5.05). As expected for a nonselective compound, AMT did not differ by more than a factor of 2.5

(pIC_{50} = 6.41, 6.48, and 6.11 for iNOS, eNOS, and nNOS, respectively). These data are summarized in Table 4.

To further validate these functional tissue experiments as reliable iNOS and eNOS models, we calculated the selectivity ratios of various standard inhibitors obtained in isolated organ models or enzymatic assays. An excellent correlation was obtained for the iNOS/eNOS selectivity ratios obtained from rat aortic experiments and those derived from enzymatic assays (Fig. 9). These data show that the potent inhibition of iNOS by BYK191023 at isolated enzymes translates into potent inhibition of iNOS in intact vascular tissue.

Discussion

The use of iNOS inhibitors as therapeutics in various diseases critically depends not just on the potency of the inhibitors but also very much on their isoform selectivity. There is general agreement that inhibition of the proinflammatory inducible isoform of NO synthases is a promising approach to treat acute as well as chronic inflammatory diseases such as septic shock, rheumatoid arthritis, and osteoarthritis. Inhibition of the endothelial NOS will disturb micro- and macro-circulatory homeostasis regulation and therefore lead to a serious deterioration of organ perfusion and other unwanted circulatory side effects. A clinical trial with the nonselective NOS inhibitor L-NMMA was stopped for those reasons (Lopez et al., 2004). Therefore, a great demand for potent and highly selective iNOS inhibitors exists to examine the role of iNOS in the above-mentioned pathophysiological and animal models. Very few highly selective iNOS inhibitors have been described in the literature, but none reached the clinic. Clinical development of 1400W was discontinued because of toxicity issues (Alderton et al., 2005). Inhibitors of iNOS dimerization only act at the monomeric level of iNOS (McMillan et al., 2000) and are not suited for inhibition of already expressed and active iNOS. Other compounds (ONO1724) are struggling with selectivity problems (Nishina et al., 2001). With BYK191023, we have identified both a potent inhibitor of the human inducible NO synthase and an inhibitor with very high selectivity versus human nNOS (200-fold) and

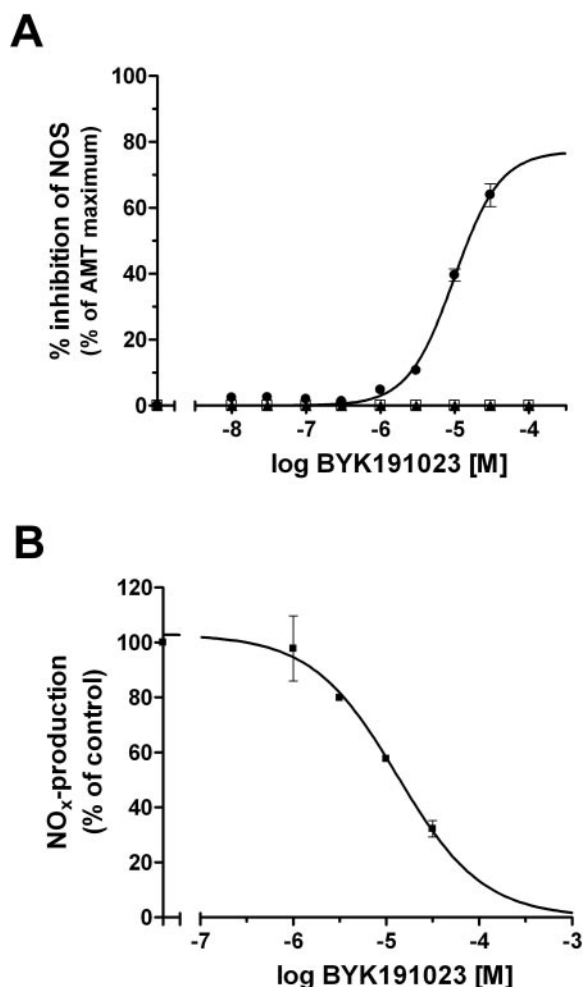


Fig. 7. BYK191023 inhibits selectively iNOS in isolated organ models. A, potency and selectivity of BYK191023 in isolated tissues using rat aorta for iNOS and eNOS and rabbit corpus cavernosum for nNOS. iNOS (●) activity was inhibited by BYK191023 with an IC_{50} of 7.9 μ M. In contrast, BYK191023 shows no inhibition in the eNOS-specific (□) or in the nNOS-specific (▲) functional model up to 100 μ M. B, inhibition of iNOS by BYK191023 in rat aortic rings monitored by the Griess assay. The iNOS was stimulated in aortic rings as described, and generation of nitrite/nitrate was inhibited by BYK191023 with an IC_{50} of 13 μ M. Each data point is the mean of triplicate determinations.

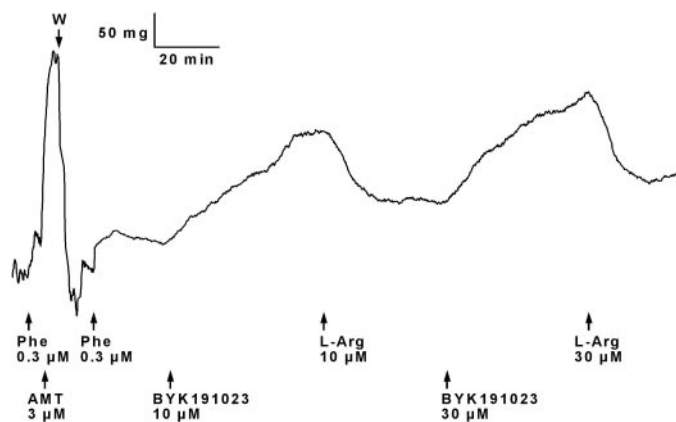


Fig. 8. iNOS inhibition at LPS-treated rat aorta. Original tracing showing the diminished contraction to phenylephrine (0.3 μ M) but full contraction by added AMT (3 μ M) because of iNOS inhibition (control). After their washout (W), the repeated contraction to phenylephrine could be partially restored and subsequently attenuated by repeated administration of increasing concentrations of BYK191023 (10 and 30 μ M) and L-arginine (10 and 30 μ M), respectively. Ordinate, milligrams of developed force of contraction.

human eNOS (>1000-fold), respectively. A K_i value of 90 nM was determined from competition experiments using increasing concentrations of L-arginine in the absence or presence of various inhibitor concentrations. This value is in close agreement to the IC_{50} value for inhibition of L-arginine-citrulline conversion in the presence of low L-arginine concentration as used in our standard protocol (86 nM). A detailed kinetic analysis of the binding mode of BYK191023 clearly showed an L-arginine-competitive mode of interaction. This is seen from the shift of IC_{50} values in the presence of increasing L-arginine concentrations (Table 2) and in the apparent K_m values of L-arginine in the presence of increasing inhibitor concentrations (Fig. 3A). The corresponding Schild plots reveal slopes near to 1, clearly indicating an L-arginine competitive mechanism for iNOS inhibition by BYK191023. An L-arginine competitive and reversible binding of BYK191023 to iNOS was further demonstrated in a functional in vitro model using isolated rat aorta. The concentration-dependent contraction of rat aorta by BYK191023 because of iNOS inhibition could strikingly be reversed by subsequent addition of increasing L-arginine concentrations (Fig. 8).

The compound is chemically unrelated to the natural substrate L-arginine. BYK191023 consists of two chemical moieties: the methoxy pyridine head group and the imidazopyridine residue linked via an ethylene bridge. It is already known that small heterocyclic compounds such as aminopicolines or imidazoles or small aliphatic compounds (isothioreas) show potent but nonselective inhibition of all NO

synthase isoforms (Chabin et al., 1996; Faraci et al., 1996). The methoxypyridine moiety is related to this structural motive, also showing potent but nonselective inhibition of NO synthases. The introduction of the ethylimidazopyridine residue leads to slightly increased potency at the inducible isoform and to the strongly pronounced selectivity of the compound BYK191023. A similar but less dramatic increase of selectivity was seen linking the 2-aminopicoline or BYK205516 moiety to the imidazopyridine (BYK237007). The imidazopyridine residue itself shows no measurable affinity, but it seems to force the inhibitor into an isoform-selective position.

Both iNOS and eNOS have been crystallized. By comparison of the reported amino acid sequence for both isoforms surrounding the active site, particularly D382 differs between iNOS and eNOS and could be responsible for the different affinities seen for iNOS and eNOS (Fischmann et al., 1999; Flinspach et al., 2004). In line with our data, a recent publication describes an increase in the selectivity of iNOS inhibition, especially over eNOS inhibition by *N*-substitution of aminopyridine (Connolly et al., 2004).

The proximity of the substrate and BH_4 binding site could theoretically lead to an influence of BH_4 binding by our inhibitors. This seems not to be the cause of potency or isoform selectivity of BYK191023 because increasing amounts of BH_4 did not protect the NOS isoforms from inhibition by BYK191023 (data not shown). However, the molecular basis for the high isoform selectivity of BYK191023 remains unknown and further investigations using NOS crystal structures with BYK191023 will be performed. Isoform-specific sequence differences of human NOS interacting with the imidazo[4,5-*b*]pyridine residue of BYK191023 are considered to be potentially responsible for the remarkable isoform selectivity. In addition to the sequence differences in D366 (eNOS) and D601 (nNOS) compared with D382 (iNOS) in the region close to the imidazopyridine, S246 (eNOS) and S481 (nNOS) are different from A262 in iNOS.

Radioligand binding data with [3H]BYK191023 in crude cytosolic fractions from iNOS-overexpressing Sf9 cells identified a single homogeneous binding site as demonstrated by the monophasic radioligand saturation curves. Association to and dissociation of [3H]BYK191023 from its binding site are again monophasic and in agreement with a single homogeneous binding site (data not shown). The identification of this binding site as iNOS is not only because it is labeled specifically by the tritiated iNOS inhibitor BYK191023 but also because the affinity of BYK191023 for its binding site is in the range of the inhibitory potency of the compound toward iNOS. Furthermore, competition experiments with selective and nonselective NOS inhibitors clearly showed the expected behavior for an interaction with iNOS. In addition, besides the use of a crude cytosolic fraction in radioligand binding assays, we confirmed specific binding of BYK191023 in direct interaction studies using surface plasmon resonance spectroscopy with the murine oxygenase domain of iNOS. The use of the murine oxygenase domain was necessary because of the demand of high surface density of thoroughly purified enzyme on the chip to obtain satisfactory signals.

BYK191023 showed a 5-fold weaker affinity toward iNOS (determined by radioligand experiments) than potency to inhibit enzymatic activity. Using our standard method, we have previously shown a clear correlation between inhibition

TABLE 4

Potencies of drugs for inhibition of iNOS and eNOS in rat thoracic aorta and of nNOS in field-stimulated rabbit corpus cavernosum
Given are pIC_{50} values with percentage of maximal inhibitory effect (%MIE) for the drugs derived from their individual half-maximal effects (means \pm S.E.M.; $n = 10-16$).

Compound	iNOS	eNOS	nNOS
	<i>M</i> (% MIE)		
BYK191023	5.14 \pm 0.04 (64)	<4.00	<4.00
L-NIL	6.03 \pm 0.03 (90)	4.90 \pm 0.03 (94)	4.58 \pm 0.08 (74)
L-NAME	4.01 \pm 0.03 (38)	5.56 \pm 0.02 (100)	5.05 \pm 0.03 (96)
AMT	6.41 \pm 0.04 (100)	6.48 \pm 0.03 (100)	6.11 \pm 0.04 (90)

L-NAME, *N*^ω-nitro-L-arginine methyl ester.

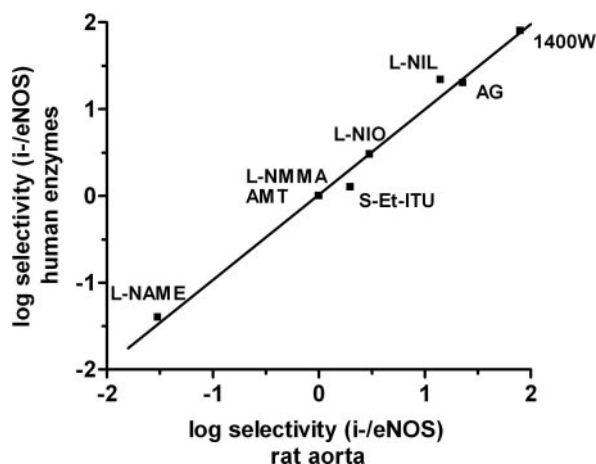


Fig. 9. Correlation of iNOS/eNOS selectively in enzymatic assays versus isolated organ models. The selectivity of various standard inhibitors in the enzymatic assay using human NOS isoforms was plotted against iNOS/eNOS selectivity of the same standard inhibitors in the NOS models using isolated rat aortic rings (correlation coefficient $r^2 = 0.988$; $p < 0.001$).

of iNOS activity and inhibition of radioligand binding with [^3H]2-aminopicoline as radioligand (Boer et al., 2000). The reason, however, for the 5-fold difference seen with BYK191023 remains unclear. An explanation for this result might be that BYK191023 inhibits the enzyme according to an irreversible mechanism or inactivation of the iNOS, although the present data argue more for a reversible inhibitory mechanism. An irreversible mechanism has been shown for other iNOS inhibitors previously (e.g., 1400W) (Garvey et al., 1997; Zhu et al., 2005) and L-NIL (Wolff et al., 1998). Further causes for the mechanistic properties of BYK191023 are presently under investigation.

The inhibitory potency of BYK191023 at iNOS drops significantly from 86 nM in the enzymatic assay to low micromolar values in the various cellular assays. This 40- to 100-fold difference is an important issue for the in vivo use of the compound and is caused by different L-arginine concentrations present in the radioactive enzymatic assay and in the cellular test systems. This drop in potency is in agreement with the loss of potency seen at the isolated enzyme in the presence of increasing L-arginine concentrations. The L-arginine concentrations in the enzymatic assay are approximately 3 to 5 μM , whereas in cellular assays the concentration in the medium is approximately 400 μM . This 100-fold difference in L-arginine concentrations will also influence the IC_{50} values in the cellular experiments. Increasing L-arginine concentrations in the radioactive enzymatic assay up to 100 μM led to comparable IC_{50} values between isolated iNOS enzyme and cellularly expressed iNOS (Table 2). A similar loss of potency is seen in LPS-pretreated rat aorta in which the intracellular L-arginine concentration competing with an inhibitor remains unknown. Again as for the cellular systems, high cellular L-arginine concentrations are probably responsible for the reduced inhibitory potency. Nevertheless, cellular potency of BYK191023 varies among different cell lines significantly. Therefore, we determined the intracellular L-arginine concentration of three cell lines used in our study. Within RAW and HEK293/iNOS cells, the L-arginine concentration was significantly reduced by more than 50% during induction of iNOS. We were surprised that the levels of L-arginine in rat mesangial cells did not change upon iNOS stimulation (data not shown). Thus, the higher cellular L-arginine levels of RMCs may explain the lower potency of L-arginine competitive inhibitors such as BYK191023.

In addition, we also examined the influence of BYK191023 on cell viability using the MTT assay. However, even cells exposed to high micromolar concentrations of BYK191023 did not show any changes in dehydrogenase activity. Therefore, BYK191023 represents a valuable tool substance for in vivo studies.

Serum binding is an important issue for the development of pharmacologically active compounds designed for clinical use. Desirably drugs show only minor serum binding properties. We determined the serum-binding capacity of BYK191023 in cellular assays. By adding human serum to the cellular HEK293 assay, we could show that the potency of BYK191023 has insignificantly decreased. Thus, we conclude that BYK191023 has only weak serum binding.

To answer the question whether the enzymatic selectivity for iNOS over eNOS is maintained at the cellular or whole organ level, we determined the potency and selectivity of BYK191023 in the LPS-treated or untreated rat aorta as

highly integrated tissue models for iNOS and eNOS. An excellent correlation between iNOS/eNOS selectivity data obtained in enzymatic assays and the in vitro functional organ models was found. A similar comparison of iNOS/nNOS selectivity was not possible because of weak or no nNOS selectivity of most NOS inhibitors.

In conclusion, BYK191023 is representative for a new class of iNOS inhibitors. BYK191023 inhibits iNOS with high selectivity in enzymatic and cellular models. Furthermore, the compound is potent in in vitro pharmacological models. Because the compound is active in vivo in various rodent models (M. D. Lehner, D. Marx, R. Boer, A. Strub, C. Hesslinger, M. Eltze, W. R. Ulrich, F. Schwoebel, R. T. Schermuly, and J. Barsig, manuscript in preparation), it represents a promising new candidate for clinical development.

Acknowledgments

We thank Dr. D. Stuehr (Cleveland Clinic Foundation, Cleveland, OH) for purified murine iNOS and iNOSox; and T. Geppert, T. Grebe, S. Haas, J. Keller, and C. Motz for expert technical assistance.

References

- Alderton WK, Angell AD, Craig C, Dawson J, Garvey E, Moncada S, Monkhous J, Rees D, Russel RJ, Schwartz S, et al. (2005) GW274150 and GW273629 are potent and highly selective inhibitors of inducible nitric oxide synthase in vitro and in vivo. *Br J Pharmacol* 145:301–312.
- Alderton WK, Cooper CE, and Knowles RG (2001) Nitric oxide synthases: structure, function and inhibition. *Biochem J* 357:593–615.
- Beaton H, Hamley P, Nicholls DJ, Tinker AC, and Wallace AV (2001) 3,4-Dihydro-1-isoquinolinamines: a novel class of nitric oxide synthase inhibitors with a range of isoform selectivity and potency. *Bioorg Med Chem Lett* 11:1023–1026.
- Blasko E, Glaser CB, Devlin JJ, Xia W, Feldman RI, Polokoff MA, Philips GB, Whitlow M, Auld DS, McMillan K, et al. (2002) Mechanistic studies with potent and selective inducible nitric-oxide synthase dimerization inhibitors. *J Biol Chem* 277:295–302.
- Boer R, Ulrich WR, Klein T, Mirau B, Haas S, and Baur I (2000) The inhibitory potency and selectivity of arginine substrate site nitric-oxide synthase inhibitors is solely determined by their affinity toward the different isoenzymes. *Mol Pharmacol* 58:1026–1034.
- Butt E, Bernhardt M, Smolenski A, Kotsonis P, Frohlich LG, Sickmann A, Meyer HE, Lohmann SM, and Schmidt HH (2000) Endothelial nitric-oxide synthase (type III) is activated and becomes calcium independent upon phosphorylation by cyclic nucleotide-dependent protein kinases. *J Biol Chem* 275:5179–5187.
- Chabin RB, McCaully E, Calaycay JR, Kelly TM, MacNaul KL, Wolfe GC, Hutchinson NI, Madhusudanaraju S, Schmidt JA, Kozarich JW, et al. (1996) Active-site structure analysis of recombinant human inducible nitric oxide synthase using imidazole. *Biochemistry* 35:9567–9575.
- Connolly S, Aberg A, Arvai A, Beaton HG, Cheshire DR, Cook AR, Cooper S, Cox D, Hamley P, Mallinder P, et al. (2004) 2-aminopyridines as highly selective inducible nitric oxide synthase inhibitors. Differential binding modes dependent on nitrogen substitution. *J Med Chem* 47:3320–3323.
- Denizot F and Lang R (1986) Rapid colorimetric assay for cell growth and survival. Modifications to the tetrazolium dye procedure giving improved sensitivity and reliability. *J Immunol Methods* 89:271–277.
- Eltze M, Grebe T, König H, Haas S, Mirau B, Baur I, Klein T, and Boer R (1999) The inducible: neuronal nitric oxide synthase (i/n-NOS) selectivity of NOS-inhibitors in rat aorta versus rabbit corpus cavernosum or rat gastric fundus correlates with human i- and nNOS. *Naunyn-Schmiedeberg's Arch Pharmacol* 359:R48.
- Eltze M, Klein T, Grebe T, Haas S, Mirau B, and Boer R (1998) Potency and selectivity of inhibitors of inducible and endothelial nitric oxide synthase in rat aorta correlate with human isozymes. *Naunyn-Schmiedeberg's Arch Pharmacol* 357:R49.
- Faraci WS, Nagel AA, Verdries KA, Vincent LA, Xu H, Nichols LE, Labasi JM, Salter ED, and Pettipher ER (1996) 2-Amino-4-methylpyridine as a potent inhibitor of inducible NO synthase activity in vitro and in vivo. *Br J Pharmacol* 119:1101–1108.
- Fischmann TO, Hruza A, Niu XD, Fossetta JD, Lunn CA, Dolphin E, Prongay AJ, Reichert P, Lundell DJ, Narula SK, et al. (1999) Structural characterization of nitric oxide synthase isoforms reveals striking active-site conservation. *Nat Struct Biol* 6:233–242.
- Fleming I, Gray GA, Julou-Schaeffer G, Parratt JR, and Stoclet JC (1990) Incubation with endotoxin activates the L-arginine pathway in vascular tissue. *Biochem Biophys Res Commun* 171:562–568.
- Flinspach ML, Li H, Jamal J, Yang W, Huang H, Hah JM, Gomez-Vidal JA, Litzinger EA, Siverman RB, and Poulos TL (2004) Structural basis for dipeptide amide isoform-selective inhibition of neuronal nitric oxide synthase. *Nat Struct Mol Biol* 11:54–59.
- Furfin ES, Harmon MF, Paith JE, Knowles RG, Salter M, Kiff RJ, Duffy C, Hazelwood R, Oplinger JA, and Garvey EP (1994) Potent and selective inhibition

- of human nitric oxide synthases. Selective inhibition of neuronal nitric oxide synthase by S-methyl-L-thiocitrulline and S-ethyl-L-thiocitrulline. *J Biol Chem* **269**:26677–26683.
- Garvey EP, Oplinger JA, Furfine ES, Kiff RJ, Laszlo F, Whittle BJ, and Knowles RG (1997) 1400W is a slow, tight binding and highly selective inhibitor of inducible nitric-oxide synthase in vitro and in vivo. *J Biol Chem* **272**:4959–4963.
- Habisch HJ, Gorren AC, Liang H, Venema RC, Parkinson JF, Schmidt K, and Mayer B (2003) Pharmacological interference with dimerization of human neuronal nitric-oxide synthase expressed in adenovirus-infected DLD-1 cells. *Mol Pharmacol* **63**:682–689.
- Hansel TT, Kharitonov SA, Donnelly LE, Erin EM, Currie MG, Moore WM, Manning PT, Recker DP, and Barnes PJ (2003) A selective inhibitor of inducible nitric oxide synthase inhibits exhaled breath nitric oxide in healthy volunteers and asthmatics. *FASEB J* **17**:1298–1300.
- Hobbs AJ, Higgs A, and Moncada S (1999) Inhibition of nitric oxide synthase as a potential therapeutic target. *Annu Rev Pharmacol Toxicol* **39**:191–220.
- Ignarro LJ, Bush PA, Buga GM, Wood KS, Fukuto JM, and Rajfer J (1990) Nitric oxide and cyclic GMP formation upon electrical field stimulation cause relaxation of corpus cavernosum smooth muscle. *Biochem Biophys Res Commun* **170**:843–850.
- Lopez A, Lorente JA, Steingrub J, Bakker J, McLuckie A, Willats S, Brockway M, Anzueto A, Holzapfel L, Breen D, et al. (2004) Multiple-center, randomized, placebo-controlled, double-blind study of the nitric oxide synthase inhibitor 546C88: effect on survival in patients with septic shock. *Crit Care Med* **32**:21–30.
- Marletta MA, Hurshman AR, and Rusche KM (1998) Catalysis by nitric oxide synthase. *Curr Opin Chem Biol* **2**:656–663.
- McCall TB, Feelisch M, Palmer RM, and Moncada S (1991) Identification of N-iminoethyl-L-ornithine as an irreversible inhibitor of nitric oxide synthase in phagocytic cells. *Br J Pharmacol* **102**:234–238.
- McMillan K, Adler M, Auld DS, Baldwin JJ, Blasko E, Browne LJ, Chelsky D, Davey D, Dolle RE, Eagen KA, et al. (2000) Allosteric inhibitors of inducible nitric oxide synthase dimerization discovered via combinatorial chemistry. *Proc Natl Acad Sci USA* **97**:1506–1511.
- Mete A and Connolly S (2003) Inhibitors of the NOS enzymes: a patent review. *IDrugs* **6**:57–65.
- Moncada S and Higgs EA (1995) Molecular mechanisms and therapeutic strategies related to nitric oxide. *FASEB J* **9**:1319–1330.
- Moore WM, Webber RK, Fok KF, Jerome GM, Connor JR, Manning PT, Wyatt PS, Misko TP, Tjoeng FS, and Currie MG (1996) 2-Iminopiperidine and other 2-iminoazaheterocycles as potent inhibitors of human nitric oxide synthase isoforms. *J Med Chem* **39**:669–672.
- Narayanan K, Spack L, McMillan K, Kilbourn RG, Hayward MA, Masters BS, and Griffith OW (1995) S-Alkyl-L-thiocitrullines. Potent stereoselective inhibitors of nitric oxide synthase with strong pressor activity in vivo. *J Biol Chem* **270**:11103–11110.
- Nishina K, Mikawa K, Kodoma S, and Obara H (2001) ONO1714, a new inducible nitric oxide synthase inhibitor, attenuates sepsis-induced diaphragmatic dysfunction in hamsters. *Anesth Analg* **92**:959–966.
- Schmidt HH and Walter U (1994) NO at work. *Cell* **78**:919–925.
- Southan GJ, Szabo C, and Thiemermann C (1995) Isothioureas: potent inhibitors of nitric oxide synthases with variable isoform selectivity. *Br J Pharmacol* **114**:510–516.
- Stuehr DJ, Cho HJ, Kwon NS, Weise MF, and Nathan CF (1991) Purification and characterization of the cytokine-induced macrophage nitric oxide synthase: an FAD- and FMN-containing flavoprotein. *Proc Natl Acad Sci USA* **88**:7773–7777.
- Tinker AC, Beaton HG, Boughton-Smith N, Cook TR, Cooper SL, Fraser-Rae L, Hallam K, Hamley P, McNally T, Nicholls DJ, et al. (2003) 1,2-Dihydro-4-quinazolinamines: potent, highly selective inhibitors of inducible nitric oxide synthase which show antiinflammatory activity in vivo. *J Med Chem* **46**:913–916.
- Titheradge MA (1999) Nitric oxide in septic shock. *Biochim Biophys Acta* **1411**:437–455.
- Ulrich W-R, Boer R, Marx D, Eltze M, Klein T, Nave R, Graedler U, Fuchß T, and Barsig J (2003), inventors; ALTANA Pharma AG and Ulrich W-R, assignees. Novel alkoxy-pyridine-derivates. World patent WO03080607. 2003 Oct 2.
- Vallance P and Leiper J (2002) Blocking NO synthesis: how, where and why? *Nat Rev Drug Discov* **1**:939–950.
- Wolff DJ, Lubeskie A, Gauld DS, and Neulander MJ (1998) Inactivation of nitric oxide synthases and cellular nitric oxide formation by N6-iminoethyl-L-lysine and N5-iminoethyl-L-ornithine. *Eur J Pharmacol* **350**:325–334.
- Young RJ, Beams RM, Carter K, Clark HA, Coe DM, Chambers CL, Davies PI, Dawson J, Drysdale MJ, Franzman KW, et al. (2000) Inhibition of inducible nitric oxide synthase by acetamidine derivatives of hetero-substituted lysine and homolysine. *Bioorg Med Chem Lett* **10**:597–600.
- Zhu Y, Nikolic D, Van Breemen RB, and Siverman RB (2005) Mechanism of inactivation of inducible nitric oxide synthase by amidines. Irreversible enzyme inactivation without inactivator modification. *J Am Chem Soc* **127**:858–868.

Address correspondence to: Dr. Andreas Strub, ALTANA Pharma AG, Byk-Gulden-Str. 2, 78467 Konstanz, Germany. E-mail: andreas.strub@altanapharma.com